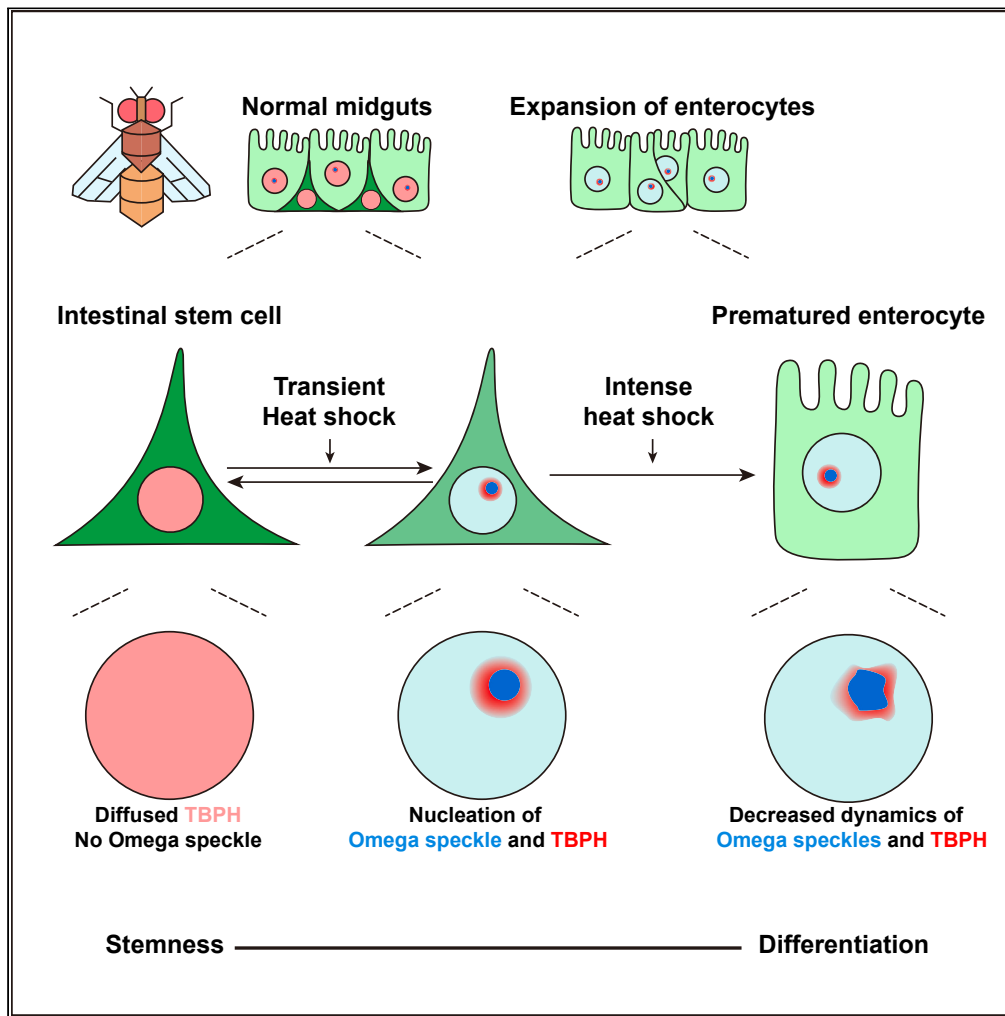


Article

Long noncoding RNAs heat shock RNA omega nucleates TBPH and promotes intestinal stem cell differentiation upon heat shock



Yinfeng Guo,
Meng Wang, Jiaxin
Zhu, Qiaoming Li,
Haitao Liu, Yang
Wang, Steven X.
Hou

w_yang@fudan.edu.cn (Y.W.)
stevenhou@fudan.edu.cn
(S.X.H.)

Highlights
LncRNA *Hsrw* is
differentially expressed in
different cell types of fly
midguts

Omega speckles nucleate
TPBH and promote the
differentiation of ISCs to
ECs

Heat shock treatment
induces the assembly of
omega speckles and
paraspeckles

Heat shock treatment
accelerates the
differentiation of fly
midguts and human iPSCs

Guo et al., iScience 27, 109732
May 17, 2024
<https://doi.org/10.1016/j.isci.2024.109732>



Article

Long noncoding RNAs heat shock RNA omega nucleates TBPH and promotes intestinal stem cell differentiation upon heat shock

Yinfeng Guo,¹ Meng Wang,¹ Jiaxin Zhu,¹ Qiaoming Li,¹ Haitao Liu,¹ Yang Wang,^{1,*} and Steven X. Hou^{1,2,*}

SUMMARY

In *Drosophila*, long noncoding RNA *Hsr ω* rapidly assembles membraneless organelle omega speckles under heat shock with unknown biological function. Here, we identified the distribution of omega speckles in multiple tissues of adult *Drosophila melanogaster* and found that they were selectively distributed in differentiated enterocytes but not in the intestinal stem cells of the midgut. We mimicked the high expression level of *Hsr ω* via overexpression or intense heat shock and demonstrated that the assembly of omega speckles nucleates TBPH for the induction of ISC differentiation. Additionally, we found that heat shock stress promoted cell differentiation, which is conserved in mammalian cells through paraspeckles, resulting in large puncta of TDP-43 (a homolog of TBPH) with less mobility and the differentiation of human induced pluripotent stem cells. Overall, our findings confirm the role of *Hsr ω* and omega speckles in the development of intestinal cells and provide new prospects for the establishment of stem cell differentiation strategies.

INTRODUCTION

In eukaryotic cells, proteins and RNAs nucleate biomolecular condensates, such as nucleoli, paraspeckles, and stress granules, via liquid-liquid phase separation.^{1–6} Nuclear condensates, also known as nuclear bodies (NBs),^{7,8} are widely expressed in different species and exhibit high diversity. The nucleation of many NBs relies on specific long noncoding RNAs (lncRNAs), such as *NEAT1_2* (nuclear paraspeckle assembly transcript 1_2) in paraspeckles, *SatIII* (Satellite III) in nuclear stress bodies, and *Hsr ω* in omega speckles (*Drosophila* exclusive).^{9–12} Most NBs act as hubs for regulating the spatial localization of RNAs and proteins and thus, participate in various biological activities.^{13,14} The dysfunction of NB assembly, localization, and structure affects cell homeostasis and results in cancer and neurodegeneration.^{15,16} Recently, several studies have revealed that NBs are also involved in cell development and differentiation. For example, the restriction of CARM1¹⁷ and TDP-43¹⁸ in paraspeckles promotes stem cell differentiation by inhibiting the expression of stem cell markers, such as OCT4 and SOX2. However, how these membraneless organelles respond to cellular stress and their relevant functions remain unknown.

Omega speckles are widely expressed in different tissues and are localized in the nucleoplasmic space close to euchromatin in *Drosophila* after exposure to heat shock.¹⁸ In omega speckles, lncRNA heat shock RNA omega (*Hsr ω*) acts as an architectural RNA (arcRNA) to initiate the assembly and maintain the stability of omega speckles. The *Hsr ω* gene locus (93D region of *Drosophila* chromatin) encodes several transcripts, including *Hsr ω -c* localized in the cytoplasm and the longer isoform *Hsr ω -n* localized in the nucleus. *Hsr ω -n* is essential for the assembly of omega speckles, while the function of *Hsr ω -c* is unknown.¹⁹ Hereafter, *Hsr ω* refers to *Hsr ω -n*. Although heat shock significantly induces the expression of *Hsr ω* , *Hsr ω* is not a canonical heat shock gene. Previous studies have reported that omega speckles are widely expressed in different developmental stages of organs, including the larval brain, wing imaginal disc, adult testis, midgut, and hindgut, and form an isolated large patch at chromosomal position 93D after heat shock.^{18,20} The constitutive expression of *Hsr ω* suggests that omega speckles may be critical for the development and survival of *Drosophila*. There is evidence that haploinsufficiency, mutation, or editing of *Hsr ω* may lead to the death of *Drosophila*.^{21,22} However, studies on how omega speckles regulate or maintain cell developmental stages and adult homeostasis are much lagged behind.

Intestinal stem cells (ISCs) are a cell population with a great capacity for self-renewal and differentiation within the epithelium of the *Drosophila* intestine.²³ They reside in the stem cell niche at the base of the intestine and interact with other intestinal cells, including enteroblasts (EBs), enterocytes (ECs), and enteroendocrine cells (EEs), to maintain the intestinal epithelium parceled by the visceral muscle.^{23,24} ISCs divide asymmetrically to generate new ISCs and EBs that eventually differentiate into ECs.²⁵ ISCs and EBs are collectively referred to as intestinal progenitor cells (IPCs).²⁶

¹State Key Laboratory of Genetic Engineering, Department of Cell and Developmental Biology at School of Life Sciences, Institute of Metabolism and Integrative Biology, Human Phenome Institute, Department of Liver Surgery and Transplantation of Liver Cancer Institute at Zhongshan Hospital, Fudan University, Shanghai 200438, China

²Lead contact

*Correspondence: w_yang@fudan.edu.cn (Y.W.), stevenhou@fudan.edu.cn (S.X.H.)

<https://doi.org/10.1016/j.isci.2024.109732>



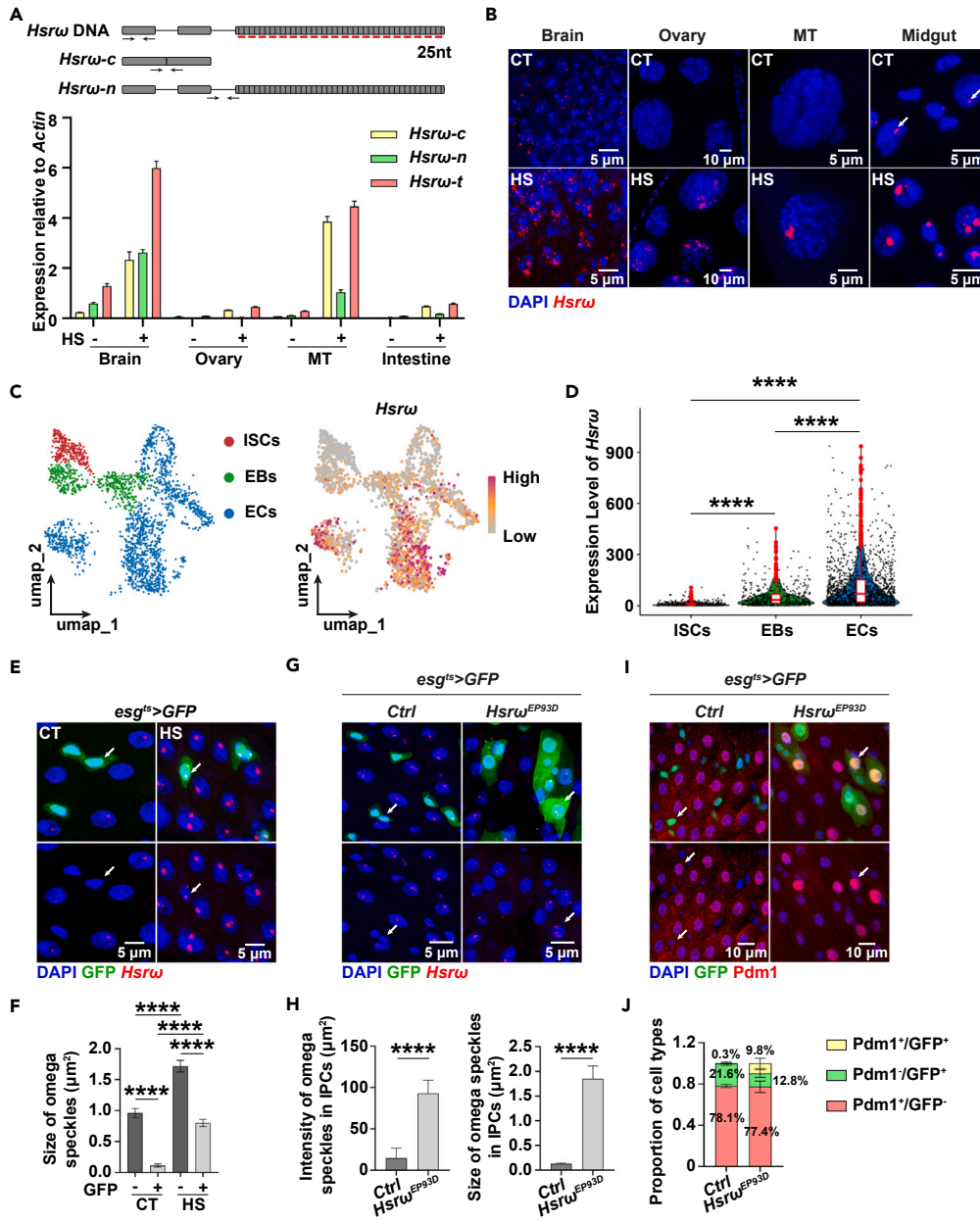


Figure 1. Omega speckles specifically distributed in ECs and overexpression of *Hsrw* promotes IPC differentiation

(A) Top, Schematic drawing of locus and the two transcripts of *Hsrw*, *Hsrw-c* here refers to the total amount of *Hsrw-n* and *Hsrw-c*. Bottom, RT-qPCR of *Hsrw* expression in brain, ovary, MT, and intestine under normal condition or heat shock ($n = 3$ independent experiments); Primers used for RT-qPCR are indicated by arrows. Red lines indicate the probes used for *Hsrw* FISH.

(B) Representative images of omega speckles in brain, ovary, MT, and midgut under normal condition or heat shock. Arrows mark large nuclei with omega speckles.

(C) The UMAP plot displays the cellular composition of total gut cells (left) and the expression of gene signatures of *Hsrw* (right).

(D) Violin plots of *Hsrw* expression in different types of cells show in panel C.

(E) Representative images of omega speckles in the posterior midgut under normal condition or heat shock. Arrows mark GFP-positive IPCs with no omega speckles.

(F) Statistics of the size of omega speckles show in panel E ($n = 417, 50, 478$ and 56).

(G) Representative images of GFP and omega speckles in posterior midguts expressing UAS-GFP alone or expressing *Hsrw*^{EP93D}. Arrows mark GFP-positive cells.

(H) Statistics of the intensity and size of omega speckles in the IPCs shows in panel G ($n = 352$ and 38).

(I) Representative images of *esg-gal4*>GFP and Pdm1 in posterior midguts expressing UAS-GFP alone or expressing *Hsrw*^{EP93D}. Arrows mark GFP-positive cells.

Figure 1. Continued

(J) Statistics of the proportion of Pdm1⁺/GFP⁺, Pdm1⁻/GFP⁺, and Pdm1⁺/GFP⁻ cells in posterior midguts in I (n = 6 guts). MT, Malpighian tubule. CT, control to HS. Ctrl, control to *Hsrw*^{EP93D}. Data in A, F–J are represented as mean ± s.d., p values in D, F and H are calculated using two-tailed unpaired Student's t test; ****p < 0.0001.

See also Figure S1.

In this study, we investigated the function of omega speckles in the development of the adult *Drosophila* midgut, which is a part of the intestine, and found that omega speckles were differentially expressed in different intestinal cell types. In the midgut, omega speckles are assembled in ECs but are absent in IPCs. Induction of *Hsrw* expression and the assembly of omega speckles promoted the differentiation of IPCs into ECs. Mechanistically, omega speckles recruited and nucleated TBPH (TDP-43 homolog) to regulate the expression of stemness genes. Taken together, our findings demonstrated the function of omega speckles in regulating the stemness-differentiation transition of IPCs via the *Hsrw*-omega speckles-TDP-43 axis during the intestinal development of *Drosophila*.

RESULTS**Identification of heat shock RNA omega expression and the distribution of omega speckles in different tissues of *Drosophila***

It has been reported that *Hsrw* is widely expressed in different tissues of *Drosophila*,¹⁸ however, whether the expression levels of *Hsrw* differ among tissues is still unclear. To understand the link between the expression of *Hsrw* and the function of omega speckles, we dissected 3-day-old *W¹¹¹⁸* (wild-type *Drosophila*) followed by RNA extraction from different tissues and performed reverse transcription (RT)-quantitative polymerase chain reaction (qPCR) to quantify the expression of *Hsrw*. Consistent with the findings of a previous study,¹⁸ *Hsrw* was expressed in various tissues, including the brain, ovary, Malpighian tubule, and midgut. Heat shock stress is a canonical method used to activate *Hsrw* expression in the research on *Hsrw* and omega speckles. We found that heat shock significantly promoted *Hsrw* expression in these tissues (Figure 1A). Moreover, the proportions of the two transcripts of *Hsrw* differed among different tissues, indicating that *Hsrw*-c expression was more sensitive than *Hsrw*-n to heat shock (Figure 1A).

As the function of *Hsrw* depends on the assembly of omega speckles, we next detected the assembly of omega speckles in different tissues. We designed fluorescence dyes coupled to probes targeting *Hsrw*-n RNA according to the conservative repeat sequences (Figure 1A, top, red).²⁷ Compared with previously used digoxigenin- or biotin-labeled probes,^{18,28–30} fluorescent probes directly label RNA with higher specificity. Consistent with the RT-qPCR results, the expression level of *Hsrw* markedly increased in the nucleus and formed larger speckles in the nucleoplasm after heat shock treatment (Figure 1B). These results collectively demonstrated that *Hsrw* is expressed and assembles into omega speckles in multiple tissues and responds to thermal stress.

Cell and nuclear sizes vary drastically between different cell types and organisms, particularly during early development.³¹ Previous studies have reported that the number of nuclear membrane organelles correlates with the size of the nucleus and further regulates human pluripotent stem cells (hPSCs) differentiation.³² Here, we also found that omega speckles were highly expressed in cells with large nuclei, especially in the midgut, and there was a positive correlation between *Hsrw* intensity and nuclear size (Figure S1A). In the *Drosophila* midgut, ISCs differentiate into ECs via EBs or directly into EEs (Figure S1B). Different intestinal cell types can be distinguished based on the expression of their signature genes. Escargot (*esg*)²⁴ and Signal-transducer and activator of transcription protein at 92E (*Stat92E*)³³ are specifically expressed in IPCs. POU domain protein 1 (*Pdm1*) was used as a marker of ECs³⁴ (Figure S1B). ECs are the only polyploid cell type with large nuclei. Thus, we aimed to investigate whether the distribution of omega speckles was distinct in different midgut cell types. To verify this, we first analyzed single-cell transcriptomic data of the *Drosophila* gut from the Fly Cell Atlas (flycellatlas.org).³⁵ As the data were annotated, we extracted and re-clustered all epithelial cells from the total gut cells via UMAP (Uniform Manifold Approximation and Projection) analysis (Figure 1C, left). Compared to ISCs, the expression of gene signatures of *Hsrw* (Figure 1C, right) and the violin plot (Figure 1D) showed that ECs tended to have a higher expression level of *Hsrw*. We next analyzed cell-specific transcriptomes in the adult *Drosophila* intestine³⁶ and the results also suggested that *Hsrw* was highly expressed in ECs and EEs, but not in IPCs (Figure S1C). We then used the IPC marker *esg* to identify cell types. By specifically driving the expression of green fluorescent protein (GFP) in IPCs using *esg^{ts}-gal4* (*esg-gal4*, *tub-gal80^{ts}*), we found that omega speckles were mainly organized in non-IPCs, and heat shock treatment-induced omega speckle assembly in different cell types (Figures 1E and 1F).

Taken together, these results indicate that although *Hsrw* is broadly expressed in multiple tissues, the assembly of omega speckles differs among different cell types. Specifically, *Hsrw* and omega speckles tended to be expressed or formed in mature differentiated ECs rather than IPCs, which suggested that *Hsrw* may play a role in stem cell differentiation.

Overexpression of heat shock RNA omega promoted the differentiation of intestinal progenitor cells into enterocytes

Based on the differential distribution of omega speckles among IPCs and differentiated ECs, we speculated that omega speckles may be involved in stemness maintenance and differentiation. Since *Hsrw* is only slightly expressed in IPCs, we used a transgenic fly strain (*EP93D*) to drive the overexpression of *Hsrw* in IPCs using *esg^{ts}-gal4*.³⁷ Fluorescence *in situ* hybridization (FISH) analysis of *Hsrw* (Figures 1G and 1H) indicated the overexpression of *Hsrw* and omega speckle assembly in the IPCs. Compared to the control group, the overexpression of *Hsrw* enlarged the nuclei of IPCs (Figure S1D). To confirm the identity of these morphologically distinct cells, we performed immunofluorescence (IF) analysis of *Pdm1* (an EC marker) in the *EP93D* fly guts to classify the differentiated cells. According to the combination of *Pdm1*

and $esg^{ts} > GFP$, we classified the cells into three types, namely $Pdm1^{+}GFP^{+}$ (differentiating ECs), $Pdm1^{-}GFP^{+}$ (IPCs and differentiating IPCs), and $Pdm1^{+}GFP^{-}$ (differentiated ECs) (Figure 1I). The quantification of these three different cell types indicated that the overexpression of *Hsrw* significantly increased the proportion of $Pdm1^{+}GFP^{+}$ cells (Figure 1J), demonstrating that the overexpression of *Hsrw* and assembly of omega speckles promoted IPC differentiation into ECs.

Collectively, these results revealed that the maturation of ECs is accompanied by high expression levels of *Hsrw* and the assembly of omega speckles, and that the expression of *Hsrw* is sufficient to promote the differentiation of IPCs.

Omega speckles nucleated TBPH and promoted intestinal progenitor cell differentiation

In mammalian cells, the spatiotemporal differential expression of *NEAT1* and the assembly of paraspeckles regulate the nuclear distribution of TDP-43 and maintain cell stemness.³⁸ Similarly, the ortholog of TDP-43, TBPH has been reported to be involved in maintaining neuronal homeostasis.³⁹ Therefore, we sought to determine whether the high expression level of *Hsrw* and the assembly of omega speckles recruited TBPH and facilitated IPC differentiation. We first investigated the distribution of TBPH in the *Drosophila* midgut. Through IF analysis of TBPH in *Drosophila* with Stat92E-GFP (an IPC marker; Figure 2A), we found that TBPH was highly expressed in ECs (Figure 2B), and the puncta-like TBPH in ECs was colocalized with omega speckles, while TBPH was localized diffusely in IPCs (Figure 2C).

The aggregation state of TDP-43 correlates with mobility and function;¹⁶ therefore, we investigated whether the nucleation of TBPH affects IPCs differentiation. In mammalian cells, only TDP-43^{ANES} (lacking nuclear export signal) forms striking nuclear bodies with significantly reduced solubility, while TDP-43^{WT} (wild-type TDP-43) and TDP-43^{ANLS} are localized diffusely in the nucleus or cytoplasm, respectively.^{16,40} We introduced these three types of TDP-43 truncates carrying a Myc tag into *Drosophila* (Figure S2A) and conducted IF analysis of both TDP-43 and endogenous TBPH in the *Drosophila* intestines. In contrast to TDP-43^{WT} and TDP-43^{ANLS}, TDP-43^{ANES} spontaneously nucleated into puncta (Figures S2B–S2E). Meanwhile, only TDP-43^{ANES} significantly affected the morphology of IPCs (Figures 2D and 2E). To further clarify whether TDP-43^{ANES} overexpression enhances IPC differentiation, we performed IF analysis of *Pdm1* in these midguts and confirmed that the TDP-43^{ANES}-induced $esg^{ts} > GFP$ -positive cells were differentiating ECs (Figures 2F and 2G). Moreover, the overexpression of TDP-43^{ANES} also significantly reduced the expression levels of *esg* and *Delta* (Figure S2F), demonstrating that the overexpression of TDP-43^{ANES} promoted IPC differentiation.

Taken together, these results suggested that TBPH was differentially expressed in IPCs and ECs, and that the nuclear accumulation of TDP-43 promoted IPC differentiation.

Heat shock-induced omega speckle assembly and promoted intestinal progenitor cell differentiation to enterocytes

Hsrw is sensitive to cellular stress and omega speckles assembly is associated with TBPH recruitment.²⁹ We next investigated whether stress-induced omega speckle assembly was capable of inducing IPC differentiation. After heat shock, omega speckles were rapidly assembled, and almost all TBPH was recruited into omega speckles in both IPCs and ECs (Figures S3A–S3C). In mammalian cells, stress promotes the formation of dynamic TDP-43 nuclear bodies, which gradually disassemble with stress removal, while long-term and continuous stress causes TDP-43 nuclear bodies to phase toward aggregates with a weakened capacity to restore liquidity.¹⁶ Based on this, we hypothesized that intense or prolonged stress may maintain the sequestration of TBPH in omega speckles and induce IPC differentiation. To test this, we used three types of thermal stress, namely, “transient” heat shock (treatment at 37°C for 1 h), “prolonged” heat shock (treatment at 37°C for 3 h), and “stronger” heat shock (treatment at 40°C for 30 min). After maturity, the flies were subjected to varying heat shock conditions once a day for 4 days (Figure S3D). The flies remained vigorous throughout the transient and prolonged heat shock, while they swooned at the end of the stronger heat shock and gradually revived after the heat shock treatment ceased. In the control group, TBPH colocalized with *Hsrw* in ECs (Figures 3A and 3B). One hour after transient heat shock, TBPH bodies disassembled and redistributed, but still colocalized with *Hsrw* in some IPCs and most ECs (Figures 3C and 3D). In contrast, both prolonged and stronger heat shock significantly enhanced the stability of omega speckles and the recruitment of TBPH in IPCs (Figures 3E–3H). Under these different modes of thermal stress, we found that prolonged and stronger heat shock significantly promoted *Hsrw* expression and omega speckle assembly (Figure S3E) and attenuated the difference in TBPH expression between IPCs and ECs (Figure S3F).

We noticed that prolonged and stronger heat shock modulated the morphology of some GFP-labeled IPCs. Thus, we used *Pdm1* to label mature ECs, and found that the prolonged and stronger heat shock treatments induce more $Pdm1^{+}/GFP^{+}$ cells (Figures 3I and 3J). Of note, more omega speckle assembly in the stronger group (Figure S3E) induced more $Pdm1^{+}/GFP^{+}$ cells than those in the prolonged group, and the knockdown of *Hsrw* resulted in a significant loss of IPCs, with or without heat shock (Figures 3K and 3L), suggesting that high expression levels of *Hsrw* and of omega speckle assembly are key factors regulating IPC differentiation. To determine the relationship between the nucleation of omega speckles and TBPH in the stemness-differentiation transition, we knocked down TBPH in IPCs and found that the loss of TBPH attenuated thermal-stress-induced IPC differentiation (Figures 3K and 3L).

Collectively, these results demonstrated that heat shock-induced omega speckle assembly and TBPH aggregation, followed by the promotion of IPC differentiation.

Heat shock promoted the spontaneous differentiation of human induced pluripotent stem cells

The paraspeckles shared several homologous proteins responsible for the assembly of these bodies with omega speckles (Figure 4A). Recent studies have revealed that the assembly of paraspeckles coordinately regulates stem cell pluripotency and differentiation by regulating the distribution of TDP-43,¹⁸ and heat shock treatment can activate *NEAT1* expression and promote paraspeckle assembly. Thus, heat shock may

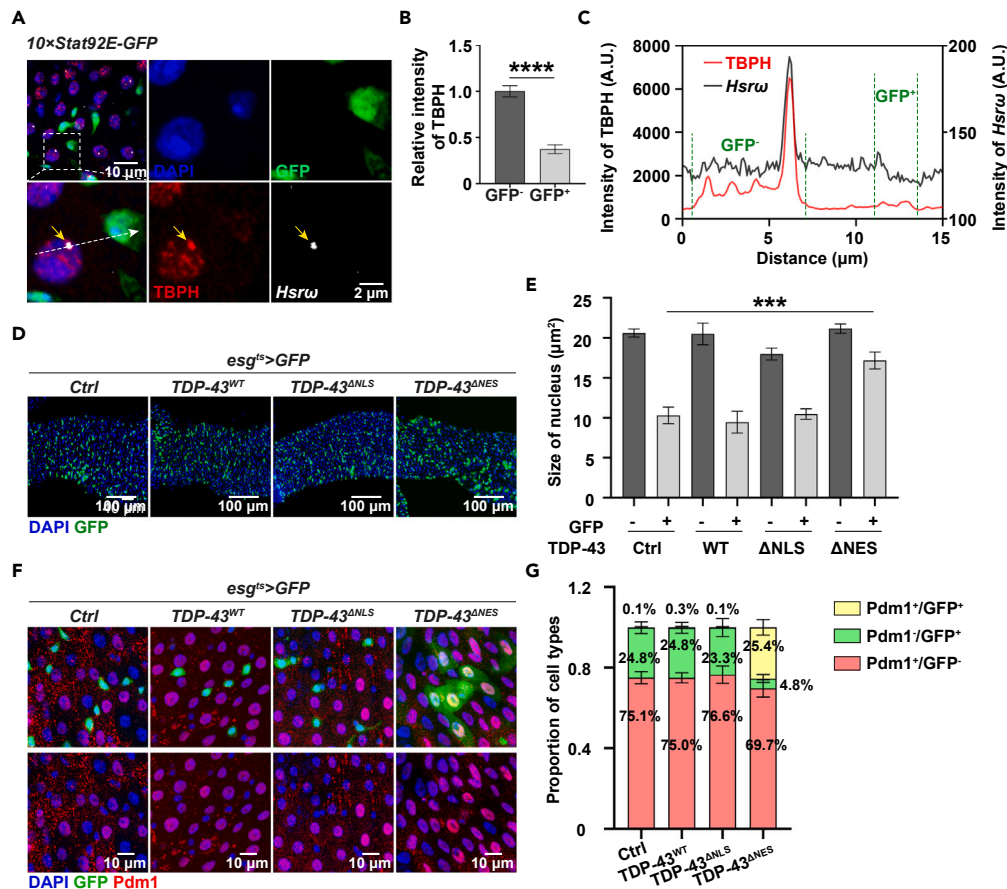


Figure 2. Overexpression of TDP-43^{ΔNES} promotes IPC differentiation

(A) Representative images of Stat92E-GFP, TBPH and omega speckles in posterior midguts. Stat92E-GFP marks IPCs. Yellow arrow marks the co-localization of omega speckle and TBPH.

(B) Statistics of the relative intensity of TBPH in GFP⁻ or GFP⁺ cells from panel A (n = 487 and 86).

(C) Line graphs of both fluorescence intensities of TBPH and Hsrw in panel A along the entire length of the dashed arrow line. GFP⁺ and GFP⁻ mark the scope of nuclei of GFP⁺ and GFP⁻ cells.

(D) Representative images of esg>GFP and omega speckles in posterior midguts expressing UAS-GFP alone or expressing human TDP-43^{WT}, TDP-43^{ΔNLS}, and TDP-43^{ΔNES}. Esg>GFP marks normal or differentiating IPCs.

(E) Statistics of nucleus sizes of GFP⁻ or GFP⁺ cells from panel D (n = 455, 53, 432, 44, 392, 62, 415, and 48 cells).

(F) Representative images of esg >GFP and Pdm1 in posterior midguts expressing GFP alone or expressing human TDP-43^{WT}, TDP-43^{ΔNLS}, and TDP-43^{ΔNES}.

(G) Statistics of the proportion of Pdm1⁺/GFP⁻, Pdm1⁻/GFP⁺, and Pdm1⁺/GFP⁺ cells in posterior midguts in panel F (n = 6 guts). Ctrl, control to TDP-43 truncations. Data in B and E are represented as mean ± s.e.m., Data in G are represented as mean ± s.d., p values in B are calculated using two-tailed unpaired Student's t test; p values in E are calculated using one-way ANOVA; ***p < 0.001, ****p < 0.0001.

See also Figure S2.

enhance the differentiation of mammalian stem cells. Here, we first reanalyzed single-cell data from the mouse⁴¹ and human intestinal tracts⁴² (Figure S4A) and then examined the expression level of NEAT1 along the developmental trajectory. Pseudo-time analysis of NEAT1 expression demonstrated that the expression level of NEAT1 increased during intestinal differentiation (Figures 4B and S4B). Notably, the long isoform of NEAT1 is an architectural RNA involved in the paraspeckle assembly. Thus, we further evaluated NEAT1 expression after the induction of the spontaneous differentiation of iPSCs. RT-qPCR results revealed that both NEAT1 and NEAT1_2 were upregulated, whereas four pluripotency markers (NANOG, OCT4, SOX2, and SSEA-4) were downregulated during the spontaneous differentiation of iPSCs (Figure 4C). We then mimicked heat shock stress in spontaneously differentiated iPSCs and found that heat shock stress-induced NEAT1 expression and paraspeckle formation (Figures S4C and S4D) and enhanced spontaneous differentiation (Figure 4D).

A previous study demonstrated that paraspeckle assembly restricts TDP-43 distribution and enhances Sox2 expression, followed by ESC differentiation.³⁸ We next wondered whether heat shock treatment affects the properties of TDP-43 and influences cell fate. Due to the low transfection efficiency of iPSCs, we transfected Emerald-fused TDP-43 into U-2 OS cells and found that TDP-43 formed much larger puncta under heat shock (Figure S4E), and these larger TDP-43 puncta exhibited poorer mobility compared with the puncta formed without heat

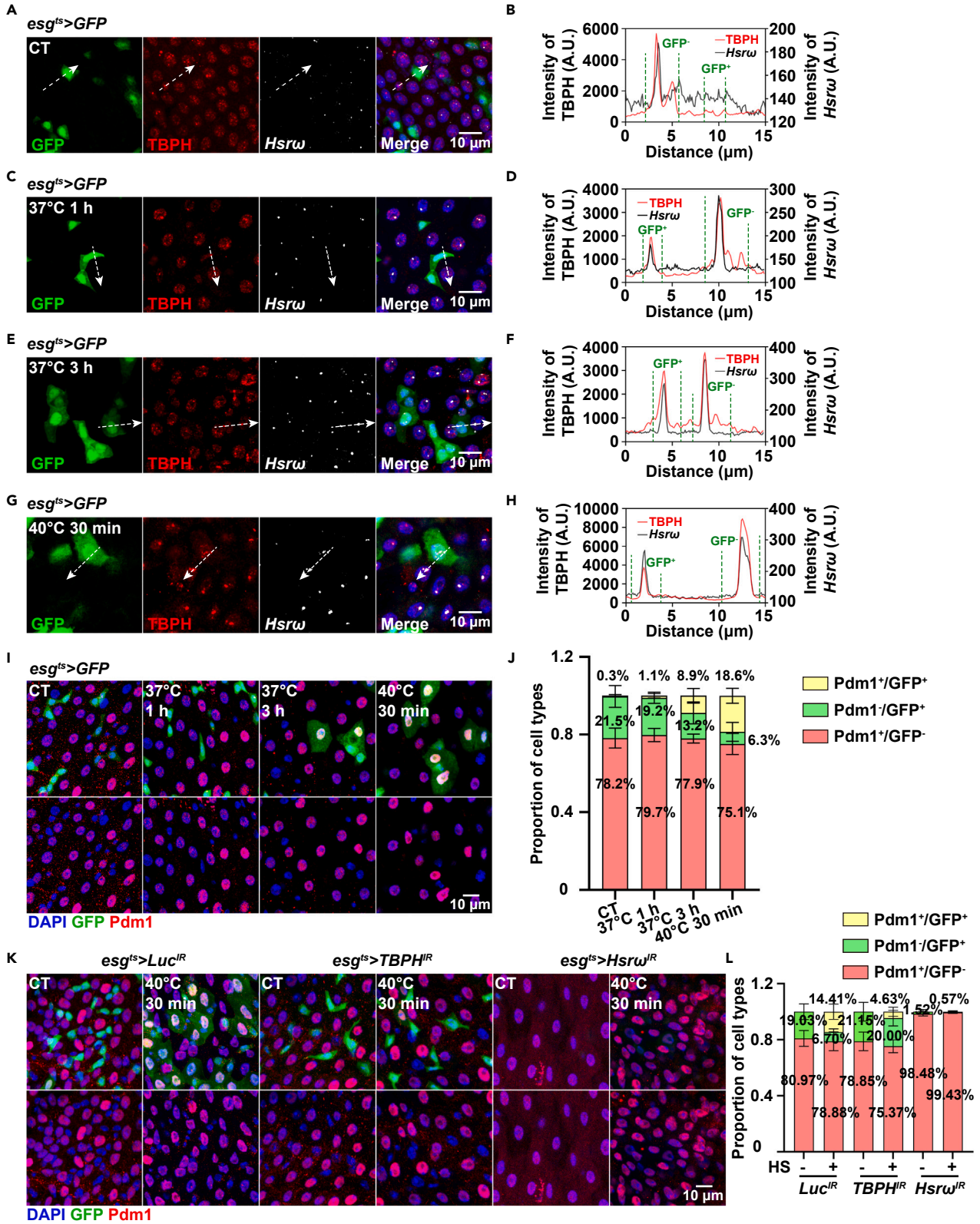


Figure 3. Intense or prolonged heat shock persists in the recruitment of TBPH at omega speckles

(A, C, E, and G) Representative images from three independent experiments of GFP, TBPH and omega speckles in posterior midguts (*esg-gal4*) expressing GFP under normal condition (A), “transient” heat shock (C), “prolonged” heat shock (E), and “stronger” heat shock (G). *Esg>GFP* marks normal or differentiating IPCs. (B, D, F, and H) Line graphs of both fluorescence intensities of TDP-43 and *Hsrw* in panels A, C, E and G along the entire length of dashed arrow lines. GFP⁺ and GFP⁻ mark the scope of nuclei of GFP⁺ and GFP⁻ cells.

(I) Representative images of *esg-gal4>GFP* and Pdm1 in posterior midguts expressing GFP under normal condition, “transient” heat shock, “prolonged” heat shock, and “stronger” heat shock.

(J) Statistics of the proportion of Pdm1⁺/GFP⁺, Pdm1⁻/GFP⁺, and Pdm1⁺/GFP⁻ cells in posterior midguts in panel I (n = 6 guts).

(K) Representative images of *esg-gal4>GFP* and Pdm1 in posterior midguts expressing *luc^{IR}* as control or expressing *TBPH^{IR}* or *Hsrw^{IR}* under normal condition and “stronger” heat shock.

(L) Statistics of the proportion of Pdm1⁺/GFP⁺, Pdm1⁻/GFP⁺, and Pdm1⁺/GFP⁻ cells in posterior midguts in panel K (n = 6 guts). CT, control to HS. Data in J and L are represented as mean ± s.d.

See also Figure S3.

shock (Figures S4F and S4G). These results suggested that the assembly of paraspeckles may restrict the mobility of TDP-43. To test whether heat shock treatment sequestered TDP-43 by promoting paraspeckle assembly, we performed dual-color imaging of TDP-43 and *NEAT1* (Figure 4E) and TDP-43 immunoprecipitation assays (Figure 4F) under spontaneous differentiation with heat shock stress. As shown in Figures 4E and 4F, spontaneous differentiation and thermal stress significantly promoted paraspeckle assembly and enhanced the interaction between TDP-43 and *NEAT1*.

Taken together, these results showed that heat shock increased the levels of *NEAT1_2* and the assembly of paraspeckles, enhancing the interaction between *NEAT1* and TDP-43 and restricting the mobility of TDP-43. This response further promoted the spontaneous differentiation of iPSCs. This is consistent with the fact that the assembly of omega speckles induced by heat shock promotes the differentiation of IPCs in *Drosophila*, suggesting that the formation of nuclear bodies may be an important event during cell differentiation, and that the induction of this process is sufficient to accelerate differentiation (Figure 4G).

DISCUSSION

Recently, many studies have demonstrated that nuclear membraneless organelles are key regulators of biological processes.^{8,43} The omega speckle is a canonical NB in *Drosophila*. Similar to other NBs, omega speckles are assembled via the architectural lncRNA *Hsrw* in most organelles and respond to various stresses. Previous studies have focused on the function of omega speckles in neurodegeneration, because of the recruitment of TBPH and Caz, the homologs of which have been well studied in human neurodegenerative diseases.^{29,44} Moreover, TBPH colocalized with omega speckles in other tissues, indicating that cross-regulation between omega speckles and TBPH may also be involved in additional biological functions. Specifically, the role of omega speckles in cell development has not yet been demonstrated.

In this study, we found that *Hsrw* was generally expressed in brains, ovaries, Malpighian tubules, and midguts by FISH and we observed that *Hsrw* was differentially expressed in different cell populations of the midgut. The adult fly midgut shows a classical mode of cell development. ISCs undergo asymmetric division to generate ISCs and EBs or pre-EE cells. EBs further differentiate into ECs, and pre-EE cells undergo differentiation to form EEs. Several key proteins involved in cell differentiation have been annotated. For example, Pdm1 is specifically expressed in ECs, while *esg*,²⁴ *Stat92E*,^{33,45} *Lin-28* and *FMRP*^{26,46} are only expressed in ISCs and EBs, which are collectively referred to as IPCs. These proteins have been shown to be responsible for stemness maintenance or the differentiation of ECs. In line with this, we found that a high expression level of *Hsrw* was sufficient to promote the assembly of omega speckles and the differentiation of IPCs to ECs and we revealed for the first time the regulatory function of *Hsrw* during cell development.

The differential expression of TBPH and colocalization between omega speckles and TBPH in ECs suggests that omega speckles are assembled in the nucleus and recruit TBPH during the differentiation of IPCs. The overexpression of TDP-43^{ANES}, which has the ability of spontaneous nucleation was sufficient to promote the differentiation of IPCs to ECs. Similarly, the stress-induced recruitment of TBPH into omega speckles induced the differentiation of IPCs into ECs. These results suggested that the nucleation of TBPH is indispensable for the differentiation of IPCs. Although the expression levels of the two stemness-related genes (*esg* and *Delta*) were downregulated after the overexpression of TDP-43^{ANES}, we have not yet determined the specific mechanism of how nucleated TBPH promotes IPCs differentiation. The sequences of RNAs in IPCs expressing different TDP-43 truncates may provide more details on the key regulators of TBPH-mediated IPC differentiation.

Unlike proteins, lncRNAs are not generally conserved among species. The sequence of *Hsrw* has undergone significant changes among multiple species within the *Drosophila* genus, but its post-transcriptional processing, major structural features, and localization remain conserved.⁴⁷ Previous studies have reported that *Hsrw* is evolutionarily conserved with *SatIII* and *NEAT1* in mammalian cells,^{9,48} *SatIII* and *Hsrw* exhibit similarities based on the presence of highly repetitive sequences and their regulation by heat shock,^{48,49} while omega speckles share similarities with paraspeckles in assembly, components, and sizes.⁷ There is also some debate regarding whether *Hsrw* and mammalian lncRNAs share direct orthologous relationships or if their similarities are merely the result of convergent evolution. Our study revealed that omega speckles nucleated by *Hsrw* recruit TBPH to promote the differentiation of IPCs, which is consistent with the role of paraspeckles in promoting ESC differentiation by sequestering TDP-43.³⁸ Therefore, our findings suggest a potential functional similarity between omega speckles and paraspeckles.

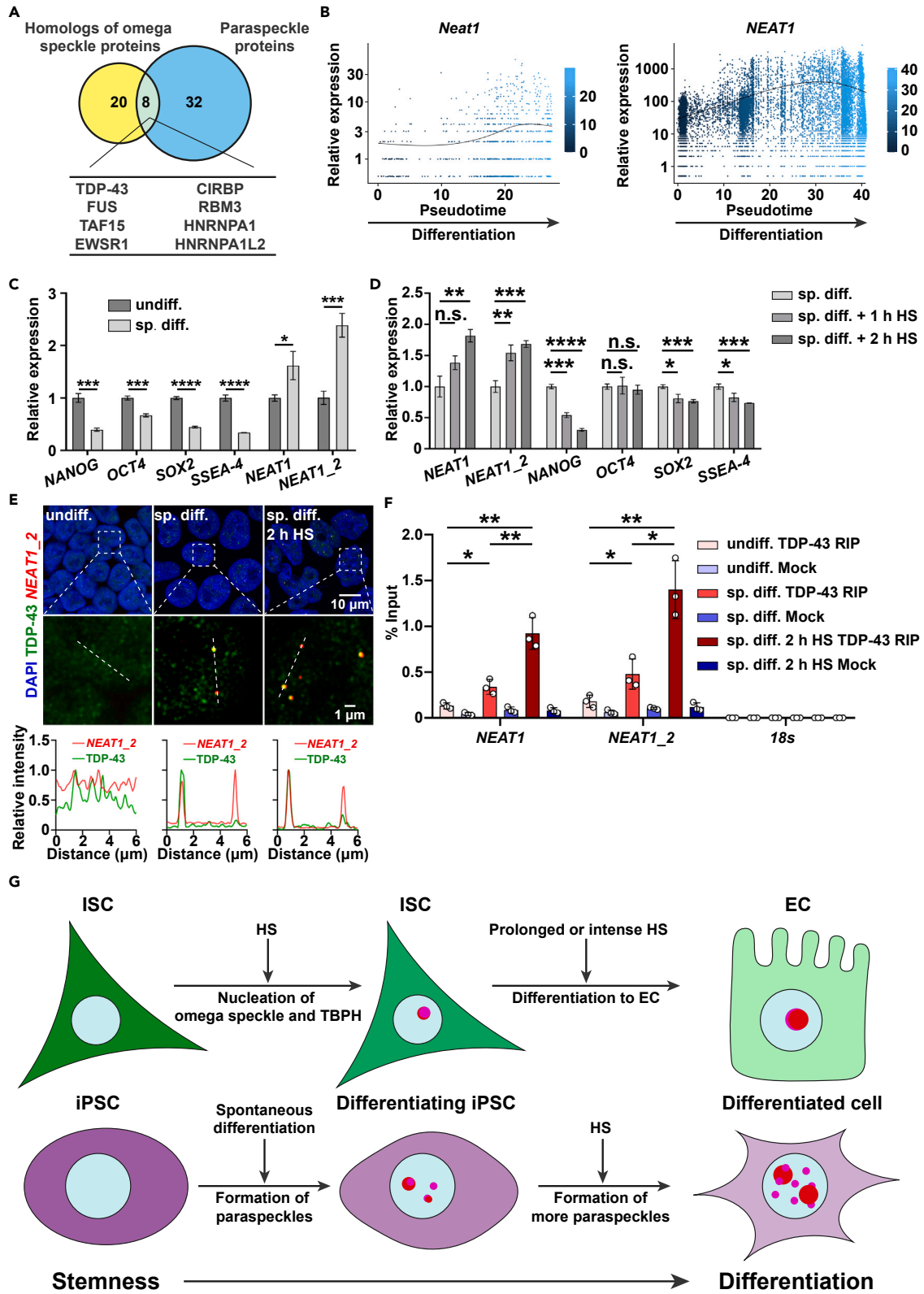


Figure 4. Heat shock accelerates the spontaneous differentiation of human iPSCs

(A) Venn diagram depicting the overlap between known paraspeckle proteins and human homologs of omega speckle proteins.

(B) The expression profile of mouse *Neat1* (left) or human *NEAT1* (right) across pseudotime.

(C) RT-qPCR determination of *NANOG*, *OCT4*, *SOX2*, *SSEA-4*, total *NEAT1*, and *NEAT1_2* expression in undifferentiated iPSCs and spontaneously differentiating cells (n = 3 independent experiments).

(D) RT-qPCR determination of total *NEAT1*, *NEAT1_2*, *NANOG*, *OCT4*, *SOX2*, and *SSEA-4* expression in spontaneously differentiating cells with or without heat shock (n = 3 independent experiments).

(E) Top, Representative images of paraspeckles and TDP-43 in undifferentiated iPSCs and spontaneously differentiating cells with or without heat shock. Bottom, Line graphs of both relative fluorescence intensities of *NEAT1_2* and TDP-43 along the entire length of dashed arrow lines on the top.

(F) Enhanced association of TDP-43 with *NEAT1_2* in undifferentiated iPSCs and spontaneously differentiating cells with or without heat shock (n = 3 independent experiments).

(G) Proposed model of heat shock promoting the differentiation of *Drosophila* IPCs and human iPSCs. See text for details. Undiff., undifferentiated iPSC. Sp. diff., spontaneously differentiating cells. RIP, RNA immunoprecipitation. Data in C, D and F are represented as mean \pm s.d., p values in C, D and F are calculated using two-tailed unpaired Student's t test; n.s., no significance, *p < 0.05, **p < 0.01, ***p < 0.001, ****p < 0.0001. See also Figure S4.

In summary, we revealed that omega speckles and the RNA-binding protein, TBPH, play critical roles in the fate determination of adult *Drosophila* intestinal cells. Nucleation of TBPH at omega speckles is a key event in the differentiation of IPCs into ECs. Overexpression of the arcRNA *Hsrw*, TDP-43^{ΔNES} or the promotion of omega speckle assembly through heat shock are capable of nucleating TBPH followed by IPC differentiation. This study provides, for the first time, insights into the functional roles of lncRNAs and nuclear bodies in cell fate determination at the organismal level, shedding new light on the study of NBs in mammals. As the digestive systems of insects and mammals are among the organs exposed to the most environmental stresses, the rapid nucleation of NBs and TDP-43 to promote ISC differentiation may be an important process to resist stress. Furthermore, considering that the dysfunction of membraneless organelles and TDP-43 has been implicated in various severe diseases, such as cancer and neurodegeneration, this work may also provide a new direction of research in studying how differences in the spatiotemporal assembly of NBs may interfere with the progression of these diseases.

Limitations of the study

In this study, we pinpoint *Hsrw* expression and omega speckles assembly as initial events to facilitate TBPH nucleation and induce ISC differentiation in response to heat shock. However, more work is needed to further characterize the mechanism and determine its universality. The rapid neogenesis of intestinal cells may be effective in resisting stress. *Hsrw* does not respond to all types of stress; thus, whether omega speckles assembly associated with TBPH nucleation is the key procedure should be further validated. We speculated that heat-shock-induced large TDP-43 puncta with low mobility restricted the function of mRNA processing, followed by cell differentiation. Although we clarified the decreased expression levels of several stem cell markers, the specific genes and relevant pathways involved require more data for confirmation.

STAR★METHODS

Detailed methods are provided in the online version of this paper and include the following:

- **KEY RESOURCES TABLE**
- **RESOURCE AVAILABILITY**
 - Lead contact
 - Materials availability
 - Data and code availability
- **EXPERIMENTAL MODEL AND STUDY PARTICIPANT DETAILS**
 - Fly strains
 - Cell culture
 - Heat shock treatment
- **METHOD DETAILS**
 - Overexpression and RNAi-mediated gene knockdown
 - Plasmid construction
 - Cell transfection
 - RNA isolation and RT-qPCR
 - Single-cell RNA sequencing (scRNA-seq) data analysis and pseudotime analysis
 - If and FISH
 - Native RNA immunoprecipitation
 - FRAP
 - Imaging analysis
- **QUANTIFICATION AND STATISTICAL ANALYSIS**

SUPPLEMENTAL INFORMATION

Supplemental information can be found online at <https://doi.org/10.1016/j.isci.2024.109732>.

ACKNOWLEDGMENTS

We thank all the members of the SL group for their comments and suggestions during the conception of this project and the development of this article. We thank Y. Fang, J. Ni, S. Hayashi, G.H. Baeg, Bloomington Drosophila Stock Center and TsingHua Fly Center for fly stocks. This work was supported by the National Natural Science Foundation of China (32200621) and the Shanghai Rising-Star Program (23QA1400600).

AUTHOR CONTRIBUTIONS

Conceptualization, Y.W. and S.X.H.; methodology, Y.W. and Y.G.; investigation, Y.G., M.W., J.X.Z., Q.M.L., and H.T.L.; writing-original draft, Y.G.; writing-review and editing, Y.W.; funding acquisition, Y.W.; resources, Y.W. and S.X.H.; supervision, Y.W. and S.X.H.

DECLARATION OF INTERESTS

The authors declare no competing financial interests.

Received: September 25, 2023

Revised: March 31, 2024

Accepted: April 9, 2024

Published: April 12, 2024

REFERENCES

- Fox, A.H., Lam, Y.W., Leung, A.K.L., Lyon, C.E., Andersen, J., Mann, M., and Lamond, A.I. (2002). Paraspeckles: a novel nuclear domain. *Curr. Biol.* 12, 13–25. [https://doi.org/10.1016/s0960-9822\(01\)00632-7](https://doi.org/10.1016/s0960-9822(01)00632-7).
- Lamond, A.I., and Spector, D.L. (2003). Nuclear speckles: a model for nuclear organelles. *Nat. Rev. Mol. Cell Biol.* 4, 605–612. <https://doi.org/10.1038/nrm1172>.
- Brangwynne, C.P., Eckmann, C.R., Courson, D.S., Rybarska, A., Hoege, C., Gharakhani, J., Jülicher, F., and Hyman, A.A. (2009). Germline P granules are liquid droplets that localize by controlled dissolution/condensation. *Science* 324, 1729–1732. <https://doi.org/10.1126/science.1172046>.
- Hernandez-Verdun, D. (2011). Assembly and disassembly of the nucleolus during the cell cycle. *Nucleus* 2, 189–194. <https://doi.org/10.4161/nucl.2.3.16246>.
- Nott, T.J., Petsalaki, E., Farber, P., Jervis, D., Fussner, E., Plochowitz, A., Craggs, T.D., Bazett-Jones, D.P., Pawson, T., Forman-Kay, J.D., and Baldwin, A.J. (2015). Phase transition of a disordered nuage protein generates environmentally responsive membraneless organelles. *Mol. Cell* 57, 936–947. <https://doi.org/10.1016/j.molcel.2015.01.013>.
- Gomes, E., and Shorter, J. (2019). The molecular language of membraneless organelles. *J. Biol. Chem.* 294, 7115–7127. <https://doi.org/10.1074/jbc.TM118.001192>.
- Mao, Y.S., Zhang, B., and Spector, D.L. (2011). Biogenesis and function of nuclear bodies. *Trends Genet.* 27, 295–306. <https://doi.org/10.1016/j.tig.2011.05.006>.
- Lacroix, E., and Audas, T.E. (2022). Keeping up with the condensates: The retention, gain, and loss of nuclear membrane-less organelles. *Front. Mol. Biosci.* 9, 998363. <https://doi.org/10.3389/fmolb.2022.998363>.
- Chujo, T., Yamazaki, T., and Hirose, T. (2016). Architectural RNAs (arcRNAs): A class of long noncoding RNAs that function as the scaffold of nuclear bodies. *Biochim. Biophys. Acta* 1859, 139–146. <https://doi.org/10.1016/j.bbagr.2015.05.007>.
- Clemson, C.M., Hutchinson, J.N., Sara, S.A., Ensminger, A.W., Fox, A.H., Chess, A., and Lawrence, J.B. (2009). An architectural role for a nuclear noncoding RNA: NEAT1 RNA is essential for the structure of paraspeckles. *Mol. Cell* 33, 717–726. <https://doi.org/10.1016/j.molcel.2009.01.026>.
- Rizzi, N., Denegri, M., Chiodi, I., Corioni, M., Valgardsdottir, R., Cobiainchi, F., Riva, S., and Biamonti, G. (2004). Transcriptional activation of a constitutive heterochromatic domain of the human genome in response to heat shock. *Mol. Biol. Cell* 15, 543–551. <https://doi.org/10.1091/mbc.e03-07-0487>.
- Dangli, A., Grond, C., Kloetzel, P., and Bautz, E.K. (1983). Heat-shock puff 93 D from *Drosophila melanogaster*: accumulation of a RNP-specific antigen associated with giant particles of possible storage function. *EMBO J.* 2, 1747–1751. <https://doi.org/10.1002/j.1460-2075.1983.tb01652.x>.
- Feric, M., Vaidya, N., Harmon, T.S., Mitrea, D.M., Zhu, L., Richardson, T.M., Kriwacki, R.W., Pappu, R.V., and Brangwynne, C.P. (2016). Coexisting Liquid Phases Underlie Nucleolar Subcompartments. *Cell* 165, 1686–1697. <https://doi.org/10.1016/j.cell.2016.04.047>.
- Hernandez-Verdun, D. (2005). Nucleolus in the spotlight. *Cell Cycle* 4, 106–108. <https://doi.org/10.4161/cc.4.1.1355>.
- Park, M.K., Zhang, L., Min, K.W., Cho, J.H., Yeh, C.C., Moon, H., Hormaechea-Agulla, D., Mun, H., Ko, S., Lee, J.W., et al. (2021). NEAT1 is essential for metabolic changes that promote breast cancer growth and metastasis. *Cell Metab.* 33, 2380–2397.e9. <https://doi.org/10.1016/j.cmet.2021.11.011>.
- Wang, C., Duan, Y., Duan, G., Wang, Q., Zhang, K., Deng, X., Qian, B., Gu, J., Ma, Z., Zhang, S., et al. (2020). Stress Induces Dynamic, Cytotoxicity-Antagonizing TDP-43 Nuclear Bodies via Paraspeckle LncRNA NEAT1-Mediated Liquid-Liquid Phase Separation. *Mol. Cell* 79, 443–458.e7. <https://doi.org/10.1016/j.molcel.2020.06.019>.
- Hupalowska, A., Jedrusik, A., Zhu, M., Bedford, M.T., Glover, D.M., and Zernicka-Goetz, M. (2018). CARM1 and Paraspeckles Regulate Pre-implantation Mouse Embryo Development. *Cell* 175, 1902–1916.e13. <https://doi.org/10.1016/j.cell.2018.11.027>.
- Prasanth, K.V., Rajendra, T.K., Lal, A.K., and Lakhotia, S.C. (2000). Omega speckles - a novel class of nuclear speckles containing hnRNPs associated with noncoding hsr-omega RNA in *Drosophila*. *J. Cell Sci.* 113, 3485–3497.
- Hogan, N.C., Traverse, K.L., Sullivan, D.E., and Pardue, M.L. (1994). The Nucleus-Limited Hsr-Omega-N Transcript Is a Polyadenylated Rna with a Regulated Intracellular Turnover. *J. Cell Biol.* 125, 21–30. <https://doi.org/10.1083/jcb.125.1.21>.
- Leader, D.P., Krause, S.A., Pandit, A., Davies, S.A., and Dow, J.A.T. (2018). FlyAtlas 2: a new version of the *Drosophila melanogaster* expression atlas with RNA-Seq, miRNA-Seq and sex-specific data. *Nucleic Acids Res.* 46, D809–D815. <https://doi.org/10.1093/nar/gkx976>.
- Mohler, J., and Pardue, M.L. (1984). Mutational Analysis of the Region Surrounding the 93d Heat Shock Locus of *DROSOPHILA MELANOGASTER*. *Genetics* 106, 249–265. <https://doi.org/10.1093/genetics/106.2.249>.
- Mallik, M., and Lakhotia, S.C. (2011). Pleiotropic consequences of misexpression of the developmentally active and stress-inducible non-coding hsromega gene in *Drosophila*. *J. Biosci.* 36, 265–280. <https://doi.org/10.1007/s12038-011-9061-x>.
- Ohlstein, B., and Spradling, A. (2006). The adult *Drosophila* posterior midgut is maintained by pluripotent stem cells. *Nature* 439, 470–474. <https://doi.org/10.1038/nature04333>.
- Micchelli, C.A., and Perrimon, N. (2006). Evidence that stem cells reside in the adult *Drosophila* midgut epithelium. *Nature* 439,

- 475–479. <https://doi.org/10.1038/nature04371>.
25. Ohlstein, B., and Spradling, A. (2007). Multipotent *Drosophila* intestinal stem cells specify daughter cell fates by differential notch signaling. *Science* 315, 988–992. <https://doi.org/10.1126/science.1136606>.
 26. Chen, C.H., Luhur, A., and Sokol, N. (2015). Lin-28 promotes symmetric stem cell division and drives adaptive growth in the adult *Drosophila* intestine. *Development* 142, 3478–3487. <https://doi.org/10.1242/dev.127951>.
 27. Garbe, J.C., Bendena, W.G., Alfano, M., and Pardue, M.L. (1986). A *Drosophila* heat shock locus with a rapidly diverging sequence but a conserved structure. *J. Biol. Chem.* 261, 16889–16894.
 28. Hughes, S.C., and Krause, H.M. (1999). Single and double FISH protocols for *Drosophila*. *Methods Mol. Biol.* 122, 93–101. <https://doi.org/10.1385/1-59259-722-x:93>.
 29. Lo Piccolo, L., Bonaccorso, R., Attardi, A., Li Greci, L., Romano, G., Sollazzo, M., Giurato, G., Ingrassia, A.M.R., Feiguin, F., Corona, D.F.V., and Onorati, M.C. (2018). Loss of ISWI Function in *Drosophila* Nuclear Bodies Drives Cytoplasmic Redistribution of *Drosophila* TDP-43. *Int. J. Mol. Sci.* 19, 1082. <https://doi.org/10.3390/ijms19041082>.
 30. Piskadlo, E., Eichenberger, B.T., Giorgetti, L., and Chao, J.A. (2022). Design, Labeling, and Application of Probes for RNA smFISH. *Methods Mol. Biol.* 2537, 173–183. https://doi.org/10.1007/978-1-0716-2521-7_10.
 31. Edens, L.J., White, K.H., Jevtic, P., Li, X., and Levy, D.L. (2013). Nuclear size regulation: from single cells to development and disease. *Trends Cell Biol.* 23, 151–159. <https://doi.org/10.1016/j.tcb.2012.11.004>.
 32. Grosch, M., Ittermann, S., Rusha, E., Greisle, T., Ori, C., Truong, D.J.J., O'Neill, A.C., Pertek, A., Westmeyer, G.G., and Drukker, M. (2020). Nucleus size and DNA accessibility are linked to the regulation of paraspeckle formation in cellular differentiation. *BMC Biol.* 18, 42. <https://doi.org/10.1186/s12915-020-00770-y>.
 33. Beebe, K., Lee, W.C., and Micchelli, C.A. (2010). JAK/STAT signaling coordinates stem cell proliferation and multilineage differentiation in the *Drosophila* intestinal stem cell lineage. *Dev. Biol.* 338, 28–37. <https://doi.org/10.1016/j.ydbio.2009.10.045>.
 34. Lee, W.C., Beebe, K., Sudmeier, L., and Micchelli, C.A. (2009). Adenomatous polyposis coli regulates *Drosophila* intestinal stem cell proliferation. *Development* 136, 2255–2264. <https://doi.org/10.1242/dev.035196>.
 35. Li, H., Janssens, J., De Waegeneer, M., Kolluru, S.S., Davie, K., Gardeux, V., Saelens, W., David, F.P.A., Brbić, M., Spanier, K., et al. (2022). Fly Cell Atlas: A single-nucleus transcriptomic atlas of the adult fruit fly. *Science* 375, eabk2432. <https://doi.org/10.1126/science.abk2432>.
 36. Dutta, D., Dobson, A.J., Houtz, P.L., Gläßer, C., Revah, J., Korzelius, J., Patel, P.H., Edgar, B.A., and Buchon, N. (2015). Regional Cell-Specific Transcriptome Mapping Reveals Regulatory Complexity in the Adult *Drosophila* Midgut. *Cell Rep.* 12, 346–358. <https://doi.org/10.1016/j.celrep.2015.06.009>.
 37. Mallik, M., and Lakhota, S.C. (2009). The developmentally active and stress-inducible noncoding *hsr omega* gene is a novel regulator of apoptosis in *Drosophila*. *Genetics* 183, 831–852. <https://doi.org/10.1534/genetics.109.108571>.
 38. Modic, M., Grosch, M., Rot, G., Schirge, S., Lepko, T., Yamazaki, T., Lee, F.C.Y., Rusha, E., Shaposhnikov, D., Palo, M., et al. (2019). Cross-Regulation between TDP-43 and Paraspeckles Promotes Pluripotency-Differentiation Transition. *Mol. Cell* 74, 951–965.e13. <https://doi.org/10.1016/j.molcel.2019.03.041>.
 39. Park, J.H., Chung, C.G., Park, S.S., Lee, D., Kim, K.M., Jeong, Y., Kim, E.S., Cho, J.H., Jeon, Y.M., Shen, C.K.J., et al. (2020). Cytosolic calcium regulates cytoplasmic accumulation of TDP-43 through Calpain-A and Importin alpha3. *Elife* 9, e60132. <https://doi.org/10.7554/eLife.60132>.
 40. Ayala, Y.M., Zago, P., D'Ambrogio, A., Xu, Y.F., Petrucelli, L., Buratti, E., and Baralle, F.E. (2008). Structural determinants of the cellular localization and shuttling of TDP-43. *J. Cell Sci.* 121, 3778–3785. <https://doi.org/10.1242/jcs.038950>.
 41. Xiao, L., Warner, B., Mallard, C.G., Chung, H.K., Shetty, A., Brantner, C.A., Rao, J.N., Yochum, G.S., Koltun, W.A., To, K.B., et al. (2023). Control of Paneth cell function by HuR regulates gut mucosal growth by altering stem cell activity. *Life Sci. Alliance* 6, e202302152. <https://doi.org/10.26508/lsa.202302152>.
 42. Zeve, D., Stas, E., de Sousa Casal, J., Mannam, P., Qi, W., Yin, X., Dubois, S., Shah, M.S., Syverson, E.P., Hafner, S., et al. (2022). Robust differentiation of human enteroendocrine cells from intestinal stem cells. *Nat. Commun.* 13, 261. <https://doi.org/10.1038/s41467-021-27901-5>.
 43. Banani, S.F., Lee, H.O., Hyman, A.A., and Rosen, M.K. (2017). Biomolecular condensates: organizers of cellular biochemistry. *Nat. Rev. Mol. Cell Biol.* 18, 285–298. <https://doi.org/10.1038/nrm.2017.7>.
 44. Lo Piccolo, L., Jantrapirom, S., Nagai, Y., and Yamaguchi, M. (2017). FUS toxicity is rescued by the modulation of lncRNA *hsr omega* expression in *Drosophila melanogaster*. *Sci. Rep.* 7, 15660. <https://doi.org/10.1038/s41598-017-15944-y>.
 45. Liu, W., Singh, S.R., and Hou, S.X. (2010). JAK-STAT is restrained by Notch to control cell proliferation of the *Drosophila* intestinal stem cells. *J. Cell. Biochem.* 109, 992–999. <https://doi.org/10.1002/jcb.22482>.
 46. Luhur, A., Buddika, K., Ariyapala, I.S., Chen, S., and Sokol, N.S. (2017). Opposing Post-transcriptional Control of lncR by FMRP and LIN-28 Adjusts Stem Cell-Based Tissue Growth. *Cell Rep.* 21, 2671–2677. <https://doi.org/10.1016/j.celrep.2017.11.039>.
 47. Sahu, R.K., Mutt, E., and Lakhota, S.C. (2020). Conservation of gene architecture and domains amidst sequence divergence in the *hsr omega* lncRNA gene across the *Drosophila* genus: an in silico analysis. *J. Genet.* 99, 64.
 48. Chung, C.Y., Berson, A., Kennerdell, J.R., Sartoris, A., Unger, T., Porta, S., Kim, H.J., Smith, E.R., Shilatfard, A., Van Deerlin, V., et al. (2018). Aberrant activation of non-coding RNA targets of transcriptional elongation complexes contributes to TDP-43 toxicity. *Nat. Commun.* 9, 4406. <https://doi.org/10.1038/s41467-018-06543-0>.
 49. Jolly, C., and Lakhota, S.C. (2006). Human sat III and *Drosophila* *hsr omega* transcripts: a common paradigm for regulation of nuclear RNA processing in stressed cells. *Nucleic Acids Res.* 34, 5508–5514. <https://doi.org/10.1093/nar/gkl711>.
 50. Goto, S., and Hayashi, S. (1999). Proximal to distal cell communication in the *Drosophila* leg provides a basis for an intercalary mechanism of limb patterning. *Development* 126, 3407–3413. <https://doi.org/10.1242/dev.126.15.3407>.
 51. Ayala-Camargo, A., Ekas, L.A., Flaherty, M.S., Baeg, G.H., and Bach, E.A. (2007). The JAK/STAT pathway regulates proximo-distal patterning in *Drosophila*. *Dev. Dyn.* 236, 2721–2730. <https://doi.org/10.1002/dvdy.21230>.
 52. Hao, Y., Hao, S., Andersen-Nissen, E., Mauck, W.M., 3rd, Zheng, S., Butler, A., Lee, M.J., Wilk, A.J., Darby, C., Zager, M., et al. (2021). Integrated analysis of multimodal single-cell data. *Cell* 184, 3573–3587.e29. <https://doi.org/10.1016/j.cell.2021.04.048>.
 53. Qiu, X., Hill, A., Packer, J., Lin, D., Ma, Y.A., and Trapnell, C. (2017). Single-cell mRNA quantification and differential analysis with Census. *Nat. Methods* 14, 309–315. <https://doi.org/10.1038/nmeth.4150>.
 54. Dundr, M., Hoffmann-Rohrer, U., Hu, Q., Grummt, I., Rothblum, L.I., Phair, R.D., and Misteli, T. (2002). A kinetic framework for a mammalian RNA polymerase *in vivo*. *Science* 298, 1623–1626. <https://doi.org/10.1126/science.1076164>.

STAR★METHODS

KEY RESOURCES TABLE

| REAGENT or RESOURCE | SOURCE | IDENTIFIER |
|--|-------------------------------|--|
| Antibodies | | |
| Rabbit anti-TDP-43 | Proteintech | Cat#10782-2-AP; RRID: AB_615042 |
| Rabbit anti-Pdm1 | Bioworld | Cat#NCP0381P |
| Goat anti-Rabbit IgG, Alexa Fluor™ 568 | Invitrogen | Cat#A-21124; RRID: AB_2535766 |
| Goat anti-Rabbit IgG, Alexa Fluor™ 647 | Invitrogen | Cat#A-21244; RRID: AB_2535812 |
| Bacterial and virus strains | | |
| DH5 α Chemically Competent Cell | Tsingke | Cat#TSC-C14 |
| Chemicals, peptides, and recombinant proteins | | |
| Agarose | ABCONE | Cat#A47902 |
| Beyozol | Beyotime | Cat#R0011 |
| Goat Serum | Beyotime | Cat#C0265 |
| Stellaris® RNA FISH Hybridization Buffer | BIOSEARCH | Cat#SMF-HB1-10 |
| Matrigel® Matrix | Corning | Cat#356234 |
| Rubber cement | Hedebio | Cat#72170 |
| Lipofectamine™ 3000 | Invitrogen | Cat#L3000015 |
| Fetal Bovine Serum (FBS) | Lonsera | Cat#s711-001s |
| mTeSR™1 | STEMCELL Technologies | Cat#85850 |
| StemPro™ Accutase™ | Thermo | Cat#A1110501 |
| Y-27632 | MedChemExpress | Cat#HY-10071 |
| Dynabeads Protein G | Invitrogen | Cat#1003D |
| IGEPAL® CA-630 | Sigma | Cat#56741 |
| PMSF | Beyotime | Cat#ST507 |
| Ribonucleoside Vanadyl Complex (RVC) | NEB | Cat#S1402S |
| All-in-one 1st Strand cDNA Synthesis SuperMix | Novoprotein | Cat#E047 |
| Dulbecco's Phosphate Buffered Saline (DPBS) | Procell | Cat#PB180329 |
| 20 \times SSC | Sigma | Cat#S6639-1L |
| 4'-6-diamidino-2-phenylindole (DAPI) | Sigma | Cat#D9542-5MG |
| DMEM | Sigma | Cat#D6429 |
| Formamide | Sigma | Cat#F9037 |
| Paraformaldehyde | Sigma | Cat#158127-500G |
| Triton™ X-100 | Sigma | Cat#T8787-250ML |
| Ethanol | Sinoreagent | Cat#10009218 |
| Isopropanol | Sinoreagent | Cat#40064360 |
| Trichloromethane | Sinoreagent | Cat#10006818 |
| ProLong™ Glass Antifade Mountant | Thermo | Cat#P36984 |
| VECTASHIELD® Antifade Mounting Medium | Vector | Cat#H-1000-10 |
| Deposited data | | |
| Original uncropped data | This paper; Mendeley data | Mendeley Data: https://doi.org/10.17632/wcyp45svkm.1 |
| scRNA raw data for <i>Drosophila</i> | Li, H. et al. ³⁵ | flycellatlas.org |
| scRNA raw data for the mouse intestinal tract | Xiao, L. et al. ⁴¹ | GEO: GSE242410 |
| scRNA raw data for the human intestinal tract | Zeve, D. et al. ⁴² | GEO: GSE178342 |

(Continued on next page)

| Continued | | |
|---|--|---|
| REAGENT or RESOURCE | SOURCE | IDENTIFIER |
| Experimental models: Cell lines | | |
| Human iPSC | National Collection of Authenticated Cell Cultures | Cat#SCSP-1301 |
| U-2 OS | ATCC | Cat#HTB-96; RRID: |
| Experimental models: Organisms/strains | | |
| <i>W¹¹¹⁸</i> | Bloomington Drosophila Stock Center (BDSC) | Strain#3605; RRID: BDSC_3605 |
| <i>esg-gal4</i> | Goto, S. et al. ⁵⁰ | N/A |
| <i>UAS-luciferase^{RNAi}</i> | BDSC | Strain#31603; RRID: BDSC_31603 |
| <i>UAS-Hsrt^{EP93D}</i> | BDSC | Strain#59614; RRID: BDSC_59614 |
| <i>UAS-TBPH^{RNAi}</i> | TsingHua Fly Center | Strain#THU0498 |
| <i>UAS-Hsrt^{RNAi}</i> | BDSC | Strain#59616; RRID: BDSC_59616 |
| <i>pBID-UASC-TDP-43-WT/Cyo</i> | Wang, C. et al. ¹⁶ | N/A |
| <i>pBID-UASC-TDP-43-NLS^{mut}/Cyo</i> | Wang, C. et al. ¹⁶ | N/A |
| <i>pBID-UASC-TDP-43-NES^{mut}/Cyo</i> | Wang, C. et al. ¹⁶ | N/A |
| <i>10x Stat-92E-GFP</i> | Ayala-Camargo et al. ⁵¹ | N/A |
| Oligonucleotides | | |
| qPCR primers | See Table S1 | N/A |
| FISH probes | See Table S1 | N/A |
| Primers for TDP-43 ^{Emerald} construct | See Table S1 | N/A |
| Recombinant DNA | | |
| pcDNA3.1-TDP-43 ^{Emerald} | This study | N/A |
| Software and algorithms | | |
| Fiji/ImageJ | NIH | https://imagej.nih.gov/ij/ |
| GraphPad Prism Software 8 | GraphPad | https://www.graphpad.com/scientificsoftware/prism/ |
| Adobe Illustrator 2023 | Adobe | https://www.adobe.com/cn/products/illustrator |
| Office 365 | Microsoft | https://www.office.com |

RESOURCE AVAILABILITY

Lead contact

Further information and requests for experimental details, resources and reagents should be directed to and will be fulfilled by the lead contact: Steven X Hou, Ph.D. (stevenhou@fudan.edu.cn).

Materials availability

This study did not generate new unique reagents.

Plasmids generated in this paper will be shared by the [lead contact](#) upon request.

Data and code availability

- This paper analyzes existing, publicly available data. These accession numbers for the datasets are listed in the [key resources table](#). The single-cell RNA sequencing data for *Drosophila* was downloaded from Fly Cell Atlas (flycellatlas.org).³⁵ The single-cell RNA sequencing data for the human intestinal tract and mouse intestinal tract were retrieved from the Gene Expression Omnibus (GEO) database under the accession numbers GSE178342⁴² and GSE242410,⁴¹ respectively. Original uncropped microscopy data have been deposited at Mendeley Data and are publicly available as of the date of publication. The DOI is listed in the [key resources table](#).
- This paper does not report original code.
- Any additional information required to reanalyze the data reported in this paper is available from the [lead contact](#) upon request.

EXPERIMENTAL MODEL AND STUDY PARTICIPANT DETAILS

Fly strains

The following fly strains were used: *W¹¹¹⁸* (BDSC3605); *UAS-Hs ω ^{EP93D}* (BDSC59614); *esg-gal4* (from *S. Hayashi*);⁵⁰ *UAS-TBPH^{RNAi}* (THU0498); *UAS-Hs ω ^{RNAi}* (BDSC59616); *pBID-UASC-TDP-43-WT*; *pBID-UASC-TDP-43-NLS-mut*; *pBID-UASC-TDP-43-NES-mut* (gift from *Y. Fang*);¹⁶ *10 \times Stat-92E-GFP (II)* (gift from *G.H. Baeg*).⁵¹ Flies were raised on standard cornmeal media at 18°C. All flies used in the experiment were three-day-old adult female.

Cell culture

U-2OS were maintained in 10 cm dishes with DMEM (Sigma) containing 10% FBS (Lonsera) and the passage was performed using trypsin (Sigma).

Human iPSCs were cultured on Matrigel-coated (Corning) 12-well plates and expanded in mTeSR1 medium (STEMCELL Technologies) with daily medium changes. Cells were digested with StemPro Accutase (Thermo) and passaged at a ratio of 1:4 - 1:8 for every 5–7 days. On the first day, cells were cultured with medium containing 10 μ M rock inhibitor (Y-27632), and the next day with rock inhibitor-free medium until the cells were passaged again. Spontaneous differentiation of iPSC was induced by replacing mTeSR1 medium with DMEM (Sigma) containing 10% FBS (Lonsera).

All cells were maintained in a humid environment at 37°C and 5% CO₂.

Heat shock treatment

If heat shock treatment was required, the flies were placed in 37°C or 40°C incubators with fresh standard cornmeal media and iPSCs were placed in 43°C incubators with the medium.

METHOD DETAILS

Overexpression and RNAi-mediated gene knockdown

To overexpress TDP-43 truncations or *Hs ω* , or knockdown TBPH in ISCs and EBs, three or four male *UAS-TDP-43*, *UAS-Hs ω ^{EP93D}*, or *UAS-TBPH^{RNAi}* were crossed with six to eight female virgins of *esg^{ts}* at 20°C. Three-day-old adult female progenies with the appropriate genotypes were transferred to 29°C for four days before dissection.

Plasmid construction

To express TDP-43^{Emerald}, the full-length TDP-43 DNA sequence was amplified from cDNA of U-2OS cells and inserted into pEmerald-C1 vector. The primers used are listed in [Table S1](#).

Cell transfection

To express TDP-43^{Emerald} in U-2OS, cells were plated into 6-well plates 24 h before transfection, 1 μ g plasmid were transfected into U-2OS with 60–70% confluence via Lipofectamine 3000 (Invitrogen). After 24 h, cells were passaged for specific experiments.

RNA isolation and RT-qPCR

For each sample, 30 intestines, 20 brains, 20 ovaries, 50 Malpighian tubules, or all cells in 6-well plates were used. Total RNA from fly tissues or cultured cells was extracted with Beyozol (Beyotime). For RT-qPCR, cDNA was synthesized from 500 ng RNA from each sample using All-in-one 1st Strand cDNA Synthesis SuperMix (Novoprotein). qPCR was performed in a 10 μ L reaction system using SYBR Green qPCR Master Mix (Novoprotein) and CFX 96 system (BIO-RAD). *Act5* or *Actin* mRNA was used for normalization (*Act5* for fly tissues and *Actin* for cultured cells). The relative expression of each examined gene was determined by three independent experiments. The sequence of each primer was listed in [Table S1](#).

Single-cell RNA sequencing (scRNA-seq) data analysis and pseudotime analysis

For the scRNA-seq data analysis for *Drosophila*, scRNA-seq data was analyzed using Seurat in version 4.3.0,⁵² total gut cells were re-clustered as ISCs, EBs and ECs and the expression of gene signatures of *Hs ω* were visualized in UMAP plot.

For the scRNA-seq data analysis for mammalian cells, cells with fewer than 300 genes, more than 6000 genes, or more than 10% mitochondrial expression were first excluded from the analysis. Then the single-cell data were analyzed using Seurat in version 4.3.0⁵² for the downstream analysis. The pseudotime analysis was performed using Monocle 2⁵³ to investigate the developmental time and trajectory of intestinal stem cells and intestinal epithelial cells.

If and FISH

For RNA FISH, fly intestines, ovaries, brains, and Malpighian tubules were dissected in DPBS (Procell) and fixed in DPBS containing 4% formaldehyde for 30 min and then washed by DPBS for three 5 min. Fixed fly tissues were permeabilized in DPBS with 0.5% Triton X-100 (Sigma) and 1% RVC (NEB) for 30 min. Cells were seeded on 18 \times 18 mm glass coverslips (Citotest), fixed in DPBS containing 4% formaldehyde for

10 min, and permeabilized in DBPS with 0.5% Triton X-100 (Sigma) and 1% RVC (NEB) for 5 min. To visualize *Hsrw* or *NEAT1_2*, fly tissues or cells were incubated in 50% formamide (Sigma)/2× SSC (sigma) at 25°C for 10 min. Cy3/Cy5-labelled probes targeting *Hsrw* or *NEAT1_2* (the sequences of probes were listed in Table S1) were added and hybridized at 37°C in a humid dark chamber for 16 h. Unbound probes were washed out by 50% formamide/2× SSC at 37°C. Nuclei were counterstained with DAPI (Sigma) for 5 min. VECTASHIELD Antifade Mounting Medium (Vector) or ProLong Glass Antifade Mountant (Thermo) were used to mount samples. The sequence of probes was listed in Table S1.

For IF, fly intestines were dissected in DPBS and fixed in DPBS containing 4% formaldehyde for 30 min and then washed by DPBS for three 5 min. Fixed fly intestines were permeabilized in DBPS with 0.5% Triton X-100 for 30 min. Fly intestines were blocked in DBPS containing 10% goat serum at 25°C for 1 h, and then incubated with the primary antibody at 4°C overnight or at 25°C for 2 h, and next with the fluorescence-conjugated secondary antibody for 2 h at 25°C. Nuclei were counterstained with DAPI for 5 min. VECTASHIELD Antifade Mounting Medium or ProLong Glass Antifade Mountant were used to mount samples. The following antibodies were used: rabbit polyclonal anti-TDP-43 (1:100; Proteintech #10782-2-AP); rabbit polyclonal anti-Pdm1 (1:100; Bioworld #NCP0381P); Goat anti-Rabbit IgG, Alexa Fluor 568 (1:1000; Invitrogen #A-21124); Goat anti-Rabbit IgG, Alexa Fluor 647 (1:1000; Invitrogen #A-21244).

Native RNA immunoprecipitation

For each experimental group, 5×10^7 iPSCs were rinsed twice with PBS and suspended in 1 mL RNA immunoprecipitation (RIP) buffer (50 mM Tris pH 7.4, 150 mM NaCl, 0.5% Igepal, 1 mM phenylmethyl sulfonyl fluoride (PMSF)), 1× protease inhibitor cocktail (Roche) and 2 mM ribonucleoside vanadyl complex (RVC) followed by sonication. Cell lysates were centrifuged at 10,000g for 10 min at 4°C and the supernatants were precleared with 10 μ L Dynabeads Protein G (Invitrogen). The precleared supernatants were then divided into two parts equally and incubated with 20 μ L Dynabeads Protein G with 2 μ g antibodies for TDP-43 (Proteintech #10782-2-AP) or Rabbit IgG2b (Proteintech #B900610) for 2 h at 4°C, followed by washing three times with high salt buffer (RIP buffer with 0.5 M NaCl, 0.5% sodium deoxycholate and 0.1% Igepal) and twice with RIP buffer. The beads were then incubated with Beyozol (Beyotime) for RNA extraction and RT-qPCR analysis.

FRAP

For live cell imaging, U-2OS cells were cultured on 29 mm no.1.5 glass-bottomed dishes (Cellvis). Plasmid TDP-43^{Emerald} was transfected 24 h before imaging. The region of interest was photobleached and the recovery of fluorescence intensity within the region of interest was obtained for each experiment (3 prebleached images and a sequence of post-bleach images for 200 s every 5 s) on Leica TSC SP8. The fluorescence intensity of TDP-43^{Emerald} at each time point are normalized with the intensity of prebleached images and corrected relative to the unbleached regions.⁵⁴ The recovery curves are plotted and analyzed using GraphPad.

Imaging analysis

All the confocal images were taken with Zeiss LSM880 with Airyscan, Olympus FV3000, or Andor Dragonfly 200. All images in one experiment were taken using the same confocal settings. Images were cropped and processed by Fiji/ImageJ. To identify the proportions of different types of cells (such as GFP⁺ and Pdm1⁺ cells), all subtypes were counted in a 20000 μ m² area of confocal images from a similar region of each posterior midgut.

QUANTIFICATION AND STATISTICAL ANALYSIS

All data in this study were represented as mean \pm s.d. or s.e.m. Statistical analyses (two-sided Student's t test or one-way ANOVA) were performed using GraphPad Prism 8. $p < 0.05$ was considered significant. Representative images for FISH and IF were obtained from 3 independent experiments. All statistical details of experiments can be found in figure legends.